AIP Journal of Applied Physics

Dielectric resonance and magnetic properties of Fe-3% doped BaSnO3 thin films grown by pulsed laser deposition

K. Balamurugan, E. Senthil Kumar, B. Ramachandran, S. Venkatesh, N. Harish Kumar, M. S. Ramachandra Rao, and P. N. Santhosh

Citation: Journal of Applied Physics **111**, 074107 (2012); doi: 10.1063/1.3698301
View online: http://dx.doi.org/10.1063/1.3698301
View Table of Contents: http://scitation.aip.org/content/aip/journal/jap/111/7?ver=pdfcov
Published by the AIP Publishing

Articles you may be interested in

Structural and dielectric properties of laser ablated BaTiO3 films deposited over electrophoretically dispersed CoFe2O4 grains
J. Appl. Phys. **116**, 164112 (2014); 10.1063/1.4900516

Interplay between chemical state, electric properties, and ferromagnetism in Fe-doped ZnO films
J. Appl. Phys. **113**, 104503 (2013); 10.1063/1.4794882

Multifunctional behavior of ZnO supported Bi1−xDyxFeO3 nanorods
J. Appl. Phys. **110**, 054313 (2011); 10.1063/1.3636274

Influence of antiferromagnetic exchange interaction on magnetic properties of ZnMnO thin films grown pseudomorphically on ZnO (000 1 ¯) single-crystal substrates
J. Appl. Phys. **103**, 043714 (2008); 10.1063/1.2841056

Transparent and conductive oxide films with the perovskite structure: La- and Sb-doped Ba Sn O 3
J. Appl. Phys. **101**, 106105 (2007); 10.1063/1.2736629

[This article is copyrighted as indicated in the article. Reuse of AIP content is subject to the terms at: http://scitation.aip.org/termsconditions. Downloaded to] IP: 130.159.70.209 On: Fri, 05 Dec 2014 10:58:16

Dielectric resonance and magnetic properties of Fe-3% doped $BaSnO_3$ thin films grown by pulsed laser deposition

K. Balamurugan,[1,a)] E. Senthil Kumar,[1,b)] B. Ramachandran,[1] S. Venkatesh,[2]
N. Harish Kumar,[1] M. S. Ramachandra Rao,[1] and P. N. Santhosh[1,c)]
[1]*Department of Physics, Indian Institute of Technology Madras, Chennai - 600036, Tamilnadu, India*
[2]*Department of Condensed Matter Physics and Materials Science, Tata Institute of Fundamental Research, Homi Bhabha Road, Mumbai - 400005, Maharashtra, India*

(Received 17 December 2011; accepted 22 February 2012; published online 11 April 2012)

Fe-3% doped $BaSnO_3$ thin films of good crystalline quality with lattice constant $a = 4.053$ Å were grown on (2 0 0) *n*-type Si substrates by pulsed laser deposition. Micro Raman spectra of the thin films showed the presence of strain-induced Raman modes with reference to that of the bulk polycrystalline Fe-3% doped $BaSnO_3$. The films exhibited dielectric resonance in the frequency range 20 – 60 MHz and it is explained qualitatively based on the phenomenon of electromechanical piezoelectric resonance. The measured values of the resonant frequency and the surface resistivity showed a strong dependence on the thickness and the crystalline-character of the thin films. Magnetic measurements were performed selectively for the two films having (2 0 0) preferred orientation. It was found that both of them possess ferromagnetic ordering at 300 K and 1.8 K. At 300 K, the inherent diamagnetism of the undoped $BaSnO_3$ was found to be dominating for higher applied magnetic field. © *2012 American Institute of Physics*. [http://dx.doi.org/10.1063/1.3698301]

I. INTRODUCTION

The influence of lattice-strain on the physical properties of thin films due to the difference in the lattice constants of the substrate and the deposited materials has always been an interesting one. Of them, the piezoelectric and ferroelectric properties are famous. For example, $SrTiO_3$ thin films were found, using Raman spectra, to exhibit strain-induced lowering of its cubic crystal-symmetry;[1] it also exhibited ferroelectric properties at room temperature while the pure unstressed $SrTiO_3$ remains paraelectric down to 0 K.[2] $BaSnO_3$ has an ideal cubic perovskite structure belonging to the space group $Pm\bar{3}m$.[3] This semiconducting oxide was found to exhibit interesting optical and magnetic properties upon substituting a few atomic percentages of Fe or Mn for Sn in the host lattice. These centrosymmetric oxides also exhibited defect (such as oxygen vacancies and dopant ions) induced first order Raman scattering.[4,5] On the other hand, pulsed laser deposition (PLD) has been a very successful method for growing 3*d* transition (V, Cr, Mn, Fe, Co, and Ni) metal doped oxide semiconductors like ZnO, TiO_2, and SnO_2 on various substrates. Many of these thin films were found to exhibit ferromagnetism at room temperature. These are called dilute magnetic semiconducting oxide (DMS) materials.[6] Here, we report the strain-induced dielectric resonance and ferromagnetic properties of Fe-3% doped $BaSnO_3$ thin films grown on *n*-type Si substrates by PLD.

a)Current address: Department of Chemistry and Biochemistry, Duquesne University, Pittsburgh, Pennsylvania 15232, USA.
b)Current address: Department of Physics, Simon Fraser University, Burnaby, Canada.
c)Electronic mail: santhosh@physics.iitm.ac.in. Tel.: +91 44 2257 4882. Fax: +91 44 2257 4852.

II. EXPERIMENTAL DETAILS

Single phase polycrystalline $BaSn_{0.97}Fe_{0.03}O_3$ powder obtained in solid state reaction[4] was pressed into a pellet of 12 mm diameter and sintered at 1300 °C for 12 h. This sintered pellet was used as the target material for growing the Fe-3% doped $BaSnO_3$ thin films on *n*–type Si (2 0 0) substrates[7] by PLD. The deposition conditions, substrate temperature (T_s), partial pressure of oxygen (P_O), and deposition time (t) were varied, while keeping the distance between the substrate and target as constant (~5 cm), for growing polycrystalline and oriented thin films. The PLD system used in this work contains a high power (frequency tripled) pulsed Nd-YAG laser with an output of ultraviolet radiation of wavelength $\lambda = 355$ nm, power $P = 2.7$ J cm^{-2}, pulse width $w_p = 19$ ns, and repetition rate $R_r = 10$ Hz. The X-ray diffraction (XRD) data were collected using (PANalytical X'Pert Pro) X-ray diffractometer with Cu K_α radiation. Raman spectra were recorded at room temperature using a High Resolution Raman Microscope (HORIBA JOBIN YVON LabRAM HR). The approximate thickness of the films was measured using a high resolution scanning electron microscope (FEI Quanta HR-SEM). The morphology and micro-structure analysis were carried out using a scanning electron microscope (JEOL 6400 SEM) and atomic force microscope (AFM) (Veeco Metrology Group, NanoScope IV Scanning Probe Microscope). AFM images were processed using the Scanning Probe Image Processor (SPIP) 4.8.4 software package. In order to study the electrical properties, a pair of coplanar gold electrodes[8] separated by 0.2 mm distance (d), each with 1 mm length (l) and 1.5 mm width (w) were deposited on the surface of a bulk pellet and the thin films (for 7 min in a vacuum better than 10^{-5} mbar) by PLD. The dielectric properties were studied using an Impedance Analyzer (Agilent 4294 A). Measurements of electrical resistance were performed using

 © 2012 American Institute of Physics

[This article is copyrighted as indicated in the article. Reuse of AIP content is subject to the terms at: http://scitation.aip.org/termsconditions. Downloaded to] IP: 130.159.70.209 On: Fri, 05 Dec 2014 10:58:16

a Keithley 617 Programmable Electrometer. Magnetic measurements were performed using a SQUID-vibrating sample magnetometer (SVSM, Quantum Design, USA).

III. RESULTS AND DISCUSSIONS

A. Analysis of X-ray diffraction patterns

Among the many different thin film samples obtained by varying the growth parameters, three thin films (labeled as) (i) S7210, (ii) S745, and (iii) S742 were selected for further characterization based on their XRD patterns. These are the films that were grown in the conditions (i) $T_s = 700\,^\circ$C, $P_O = 20$ mbar, and $t = 10$ min, (ii) $T_s = 700\,^\circ$C, $P_O = 40$ mbar, and $t = 5$ min, and (iii) $T_s = 700\,^\circ$C, $P_O = 40$ mbar, and $t = 2$ min, respectively. The XRD patterns of the thin films S7210, S745, and S742 are shown in Fig. 1; the XRD patterns of the bulk $BaSn_{0.97}Fe_{0.03}O_3$ (Bulk Fe-3%) and *n*-type Si substrate are shown as references. (The intensity of the XRD patterns has been given in the logarithmic scale.) There is an unidentified XRD peak indicated by the ◆ symbol which is intrinsic to the substrate. Ignoring the substrate peaks, the followings are to be observed in Fig. 1: (i) the film S7210 has all the XRD peaks of bulk Fe-3% doped $BaSnO_3$ exhibiting its polycrystalline nature, (ii) the film S745 has (1 1 0) peak of negligibly very small intensity (indicated by a small circle) and a relatively high intense (2 0 0) peak, and (iii) the film S742 has only (2 0 0) peak exhibiting highly preferred growth direction. Note that the (2 0 0) peak of the Si substrate is not seen in the shown XRD pattern of S745 and S742. But, it was observed in both these films when the samples were rotated with respect to their surface normal. This rotation was carried out to get maximum intensity of XRD peaks from the deposited material, and to minimize the substrate peaks. Hence, in some specific rotation the (2 0 0) peak of Si is not seen while getting maximum intensity from the deposited material.

The lattice constant of bulk polycrystalline Fe-3% doped $BaSnO_3$ is $a_b = 4.105$ Å.[4] This is comparable with the distance between two nearest neighbor Si atoms, $a^* = 3.823$ Å of the (2 0 0) plane of Si single crystalline substrate, though the lattice constant of Si is $a = 5.406$ Å. The comparable value of a^* with a_b means a higher probability for the growth of Fe-3% doped $BaSnO_3$ thin films with the same (2 0 0) orientation of the substrate as it is shown by the XRD pattern of film S742 (see Fig. 1). The calculated lattice constant of the thin film is $a_f = 4.053$ Å. Thus there is a reduction in the lattice constant of the thin films compared with that of bulk polycrystalline Fe-3% doped $BaSnO_3$. This is due to the value of a^* being smaller than that of the bulk Fe-3% doped $BaSnO_3$. Thus Fe-3% doped $BaSnO_3$ thin films (with $a_f = 4.053$ Å) having a highly preferred (2 0 0) orientation were grown on *n*–type Si (2 0 0) substrate with $a^* = 3.823$ Å.

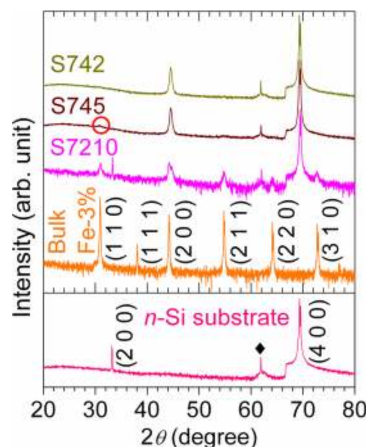

FIG. 1. X-ray diffraction patterns of thin films (S7210, S745, and S742) with reference to that of bulk Fe-3% doped $BaSnO_3$ and *n*-type Si substrate. The symbol ◆ indicates an unidentified peak which is intrinsic to the substrate.

B. Analysis of defect- and strain-induced Raman modes

Figure 2 shows the micro-Raman spectra of the Fe-3% doped $BaSnO_3$ thin films (S7210, S745, and S742) with reference to that of bulk polycrystalline Fe-3% doped $BaSnO_3$ (Bulk Fe-3%) and *n*-type Si substrate. (The intensity of the Raman spectra has been given in the logarithmic scale.) In principle, the centrosymmetric (Fe-3% doped) $BaSnO_3$ should not show first order Raman scattering.[9] But the bulk Fe-3% doped $BaSnO_3$ sample exhibit the Raman modes centered at Raman shifts 263.72, 336.36, 413.61, ∼517.37, 648.81, and 832.13 cm^{-1}. These Raman modes of bulk Fe-3% doped $BaSnO_3$ are attributed to defect-induced modes, which occur due to the local loss of translational periodicity of the lattice as an effect of the substitution of Fe-ions to Sn^{4+} ions in the host lattice and formation of oxygen vacancies.[5,10] Apart from the characteristic Raman modes of the substrate (found at ∼306.20, 524.15 cm^{-1} and a broad mode in the range 926.92 – 1010.26 cm^{-1}), the polycrystalline film S7210 exhibits Raman modes of appreciable intensity at 231.44, 306.38, ∼435.51, 483.94 cm^{-1} and a least intense mode at 684.55 cm^{-1}. Whereas the films S745 and S742 do not exhibit the least intense mode centered at 684.55 cm^{-1}. The other first four modes exhibited S7210 are found to have broadened in the case of S745 and S742 films. The mode at the lowest wave number in the (2 0 0) oriented film (S742) has split into a doublet, whose components has centered at 232.59 and 247.58 cm^{-1}. Here the degree of splitting of the fourth mode and the degree of broadening of

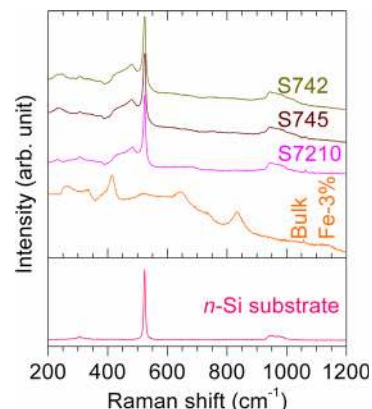

FIG. 2. Micro-Raman spectra of thin films (S7210, S745, and S742) with reference to that of bulk Fe-3% doped $BaSnO_3$ and *n*-type Si substrate.

[This article is copyrighted as indicated in the article. Reuse of AIP content is subject to the terms at: http://scitation.aip.org/termsconditions. Downloaded to] IP: 130.159.70.209 On: Fri, 05 Dec 2014 10:58:16

all four modes increase with an increase of quality of the (2 0 0) oriented crystalline-character of the films. When the Raman modes exhibited by the polycrystalline and (2 0 0) oriented thin films are compared with those exhibited by the bulk Fe-3% doped $BaSnO_3$, we have observed that one mode located immediate to the left of the high intense mode of the substrate is exclusively exhibited by the thin film samples. Considering the similarity of this specific experimental observation with the detailed investigations on the Raman spectra in epitaxial thin films of $La_{1-x}Ca_xMnO_3$ ($x = 0.33$, 0.5) grown on different substrates reported by Xiong *et al.*[11] and the observation of the first-order Raman scattering in $SrTiO_3$ thin films by Sirenko *et al.*,[1] we understand that this new mode is induced by strain in the lattice that occurred due to the difference between the *a** value of the substrate and the lattice constant of the deposited material.

C. Dielectric resonance properties

Dielectric properties were studied by measuring the in-plane capacitance (C_{ip}) of the thin films using coplanar electrode configuration. The schematic of the coplanar capacitor structure with gold electrodes used in the study is shown in Fig. 3. This coplanar capacitor configuration has a disadvantage that the derivation of the dielectric constant from the measured capacitance is difficult due to the following two reasons: (i) the electric field distribution between the coplanar electrodes is not uniform (see Fig. 3), and (ii) the surface effect is a dominant one, though the thickness of the dielectric is also influencing the capacitance. On the other hand, this kind of electrode/dielectric film/substrate type of (coplanar) capacitance structure utilizes the growth of the dielectric film directly on the substrate, which offers the advantage of having good control over crystalline quality and orientation of the dielectric film.[12] Therefore, we use the measured values of C_{ip} and the dielectric loss (tan δ) for studying the dielectric properties. For a given electrode/dielectric film/substrate coplanar capacitor, the value of C_{ip} varies as $C_{ip} \propto (l \times w)^{\alpha}/d^{\beta}$, where α and β are constants having values less than 1. The value β depends on the thickness of the dielectric film; it is higher for thicker films and vice versa.[8,13]

The frequency dependent capacitance with coplanar electrode structure (C_{ip}) and the dielectric loss (tan δ) of the thin films S7210, S745, and S742 are shown in Fig. 4. At the low frequency $f = 114.9$ Hz the C_{ip} values of the films are 0.049, 0.035, and 0.25 nF, respectively; the corresponding values of tan δ are 0.575, 0.147, and 0.883, respectively. The approximate thickness of the thin films S7210, S745, and S742 measured using cross-sectional HR-SEM images are 9.2, 2.1, and 0.8 μm, respectively. Hence, the film S745 has

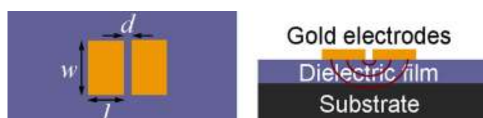

FIG. 3. Schematic views of the coplanar capacitor structure. Top view showing the dimensions (left side) and cross-sectional view showing the electric field lines through the dielectric film and the substrate (right side).

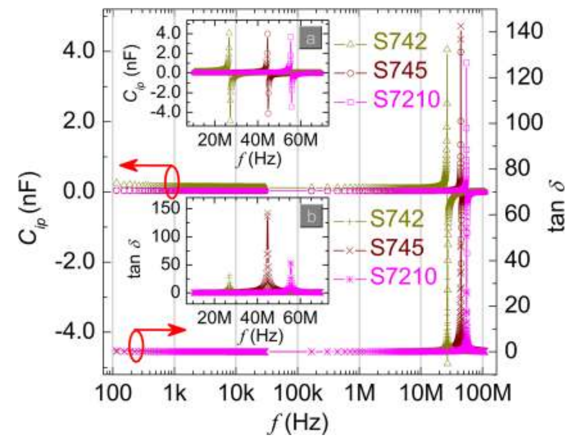

FIG. 4. Dispersion of in-plane capacitance (C_{ip}) and dielectric loss (tan δ) of the Fe-3% doped $BaSnO_3$ thin films. Dispersion of C_{ip} (inset a) and tan δ (inset b) in the dielectric resonance frequency region.

lower capacitance (nearly one order of magnitude lesser) relative to that of S742. All three films exhibit very less change in C_{ip} and tan δ over a wide range of frequency of the applied electric field. But, they exhibit abrupt changes when a particular frequency, called the resonance frequency (f_r), is reached. Each film exhibits this dielectric resonance at different frequencies. The f_r values of the films S7210, S745, and S742 are 55.43, 44.84, and 27.11 MHz, respectively (see inset a of Fig. 4); these are the values of f at which tan δ exhibits a maximum (see inset b of Fig. 4). The C_{ip} switches from a higher positive value to a higher negative value at f_r.

Following Kapustianyk *et al.*[14] we find that the observed dielectric resonance in the range of 20 – 60 MHz of applied electric field is due to the electromechanical piezoelectric resonance. The observed decrease of f_r with a decrease of the (deposition time or) thickness of the films is not in agreement with the relationship between the f_r of a piezoelectric crystal and its thickness.[15,16] This may be due to the following reasons: (i) the measurements in our experiment were carried out by using capacitors having coplanar electrodes, and (ii) as per the XRD patterns of S7210, S745, and S742 thin films, each film has a different crystalline-character. In order to

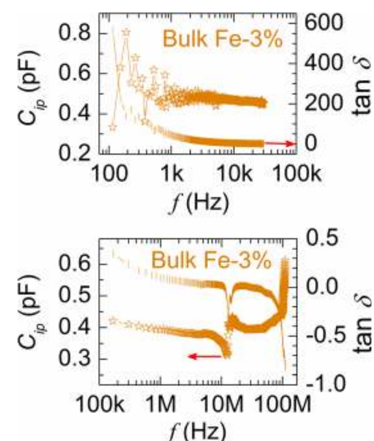

FIG. 5. Dispersion of capacitance (C_{ip}) and dielectric loss (tan δ) of the bulk Fe-3% doped $BaSnO_3$. The low frequency region and high frequency region are given in the upper and lower graphs, respectively.

[This article is copyrighted as indicated in the article. Reuse of AIP content is subject to the terms at: http://scitation.aip.org/termsconditions. Downloaded to] IP: 130.159.70.209 On: Fri, 05 Dec 2014 10:58:16

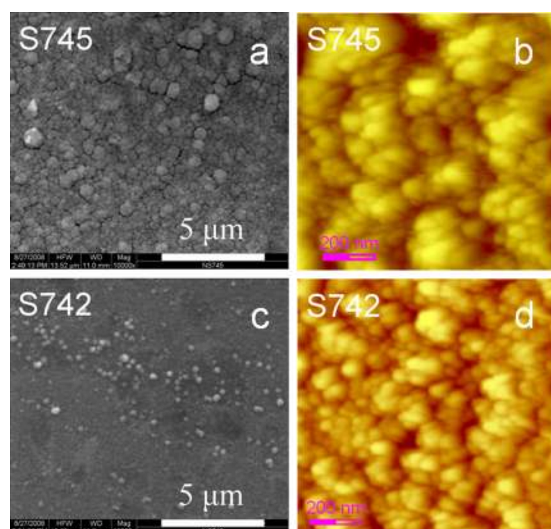

FIG. 6. The SEM (a) and (c) and AFM (b) and (d) images of S745 and S742 (Fe-3% doped $BaSnO_3$) thin films, respectively.

gain more insight on the observed dielectric resonance, the in-plane capacitance (C_{ip}) of the bulk Fe-3% doped $BaSnO_3$ pellet was measured by using the same coplanar electrode configuration. The dispersions of C_{ip} and tan δ with frequency are shown in Fig. 5. Since the changes of C_{ip} and tan δ are larger at frequencies greater than 100 kHz, the corresponding data are shown in a separate plot (bottom). As it is seen, the C_{ip} values are nearly three orders of magnitude less than what was exhibited by thin films. Moreover, bulk samples show a double resonance at the frequencies 12.81 and 14.33 MHz. Here, at the resonance frequency, the C_{ip} does not show any negative values. Hence, we believe that the lattice-strain might have induced some local-distortion in the crystal system, which should have broken the center of inversion symmetry of Fe-3% doped $BaSnO_3$ cubic crystals. This is supported by the strain-induced Raman mode observed in the thin films which was not present in bulk Fe-3% doped $BaSnO_3$. Thus, the Fe-3% doped $BaSnO_3$ thin films exhibit (deposition time or) thickness and crystalline-character dependent strain-induced dielectric resonance.

D. Surface electrical resistivity

The surface resistance (R_s) of the bulk Fe-3% doped $BaSnO_3$ pellet and the thin films were measured at room temperature, using the same coplanar electrode structure. The surface resistivity (ρ_s) was calculated using the formula $\rho_s = R_s(w/d)$ (ohm), where w is the width and d is the distance of separation of two electrodes (see Fig. 3).[17,18] The bulk sample offered a surface resistivity, $\rho_s \sim 1.1313$ MΩ for the flow of electric current. The value of ρ_s of the polycrystalline thin film S7210 is 229.09 MΩ, whereas the (2 0 0) oriented thin films S745 and S742 have ρ_s of 0.2964 MΩ and 0.1365 MΩ, respectively. The three orders of increased value of ρ_s of the polycrystalline film (S7210) should be due to the presence of grains of different crystallographic orientations and grain boundaries. Hence, the surface resistivity also shows a strong dependency on the crystalline-character of the thin films.

E. Morphology and micro structure analysis

Figures 6(a) and 6(c) show the SEM images of the thin films S745 and S742, respectively. It is seen from the SEM images that there are particles grown above the average surface of either films. These particles have wide spread size distribution. In the case of S742 there are particles of size as small as <100 nm, while the film S745 has relatively larger particles (>100 nm). Also, it is seen that these larger particles of S745 have agglomerated particles of smaller size. Figures 6(b) and 6(d) show the AFM images of the films S745 and S742, respectively. Both of the images were scanned over an area of 1 μm^2. It is seen that the grains in the samples have no regular shapes, though some of them have a nearly spherical top surface. Moreover, in either film there are grains whose top surfaces have sizes smaller than 100 nm. The estimated average, mean square roughness parameters, and maximum peak height of the S745 film are $S_a = 34.53$ nm, $S_q = 43.12$ nm, and $S_p = 101.25$ nm, respectively, whereas the values of these parameters of the S742 film are $S_a = 31.31$ nm, $S_q = 38.72$ nm, and $S_p = 107.86$ nm, respectively. These parameters indicate that the film S745 has a relatively smoother surface than S742.

F. Magnetic properties

The films S745 and S742 were selected for magnetic measurements. Figure 7(a) shows the field dependent magnetization of these samples measured at 300 and 1.8 K. Figure 7(b) shows the same data in an expanded view in the applied field range of −0.1 T to +0.1 T. It is clear that both the samples exhibit ferromagnetism at 1.8 K. At 300 K, they exhibit nonlinear variation of magnetization at a lower field

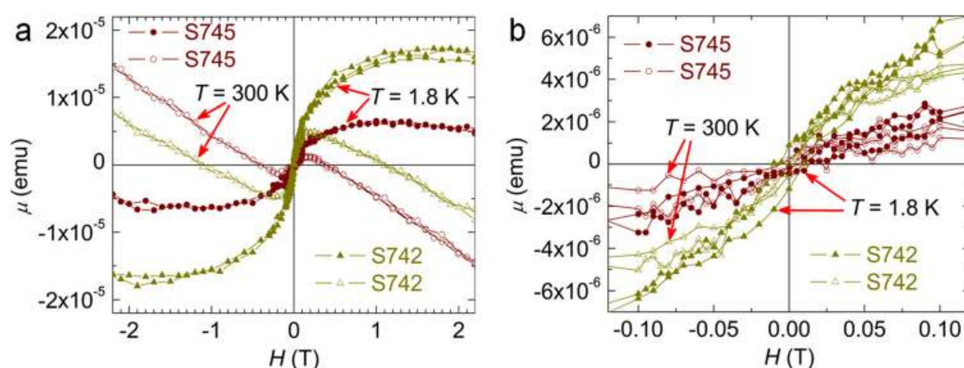

FIG. 7. (a) The field dependent magnetization of the films S745 and S742 measured at 300 K and 1.8 K temperatures. (b) An expanded view in the range of –0.1 T to +0.1 T.

[This article is copyrighted as indicated in the article. Reuse of AIP content is subject to the terms at: http://scitation.aip.org/termsconditions. Downloaded to] IP: 130.159.70.209 On: Fri, 05 Dec 2014 10:58:16

while there is a domination of diamagnetic character observed at the higher field. This agrees with our earlier observations that, at 300 K, in the case of Mn-3% doped $BaSnO_3$ bulk polycrystalline sample, the inherent diamagnetic character of the undoped $BaSnO_3$ dominates at a higher applied field.[5] Also, the ferromagnetic character of the bulk polycrystalline $BaSn_{1-x}Mn_xO_3$ (with $x = 0.01$–0.05) samples was found to increase with an increase in the dopant (Mn) concentration.[5] Hence, the observed domination of the diamagnetic character of the thin films S745 and S742 at higher applied field may be extinguished if the dopant (Fe) concentration is increased optimally. However, more investigations are required to ascertain whether the observed ferromagnetism is inherent to the sample or it comes from any secondary phases. For example, many of the Co doped TiO_2 (anatase) DMS thin films grown by PLD method exhibited ferromagnetism with high Curie temperature (T_C) 650 – 700 K. But, the observed ferromagnetism was not inherent to the materials. It was rather found to be due to the presence of the Co cluster.[19–21] Similarly, low temperature ferromagnetism ($T_C \sim 48$ K) observed in the case of Mn-doped Cu_2O thin films were due to the presence of Mn_3O_4 precipitates.[22]

IV. SUMMARY

The Fe-3% doped $BaSnO_3$ thin films grown on *n*–type Si (2 0 0) substrates by PLD were found to have either polycrystalline nature or highly preferred (2 0 0) oriented growth depending on the deposition conditions. The films exhibited strain-induced Raman modes indicating the lowering of cubic symmetry of the bulk Fe-3% doped $BaSnO_3$. The films exhibited dielectric resonance in the frequency range 20 – 60 MHz depending on their (deposition time or) thickness and crystalline-character. The observed dielectric resonance has been explained by the phenomenon of electromechanical piezoelectric resonance. Similarly, the surface electrical resistivity showed a strong dependence on the crystalline-character of the thin films. Further the films grown for 5 and 2 min were selected for microscopic investigations and magnetization studies. Analysis of AFM images showed that the film grown for 5 min has a relatively smoother surface than the film grown for 2 min. The magnetic measurements, performed at 300 K and 1.8 K, showed that both the films have ferromagnetic ordering. This ferromagnetic ordering is overcome by the inherent diamagnetic nature of $BaSnO_3$ for higher applied magnetic field at 300 K.

ACKNOWLEDGMENTS

The authors thank Mr. Krishna Surendra for his valuable help with HR-SEM.

[1] A. A. Sirenko, I. A. Akimov, J. R. Fox, A. M. Clark, Hong-Cheng Li, Weidong Si, and X. X. Xi, Phys. Rev. Lett. **82**, 4500 (1999).
[2] J. H. Haeni, P. Irvin, W. Chang, R. Uecker, P. Reiche, Y. L. Li, S. Choudhury, W. Tian, M. E. Hawley, B. Craigo, A. K. Tagantsev, X. Q. Pan, S. K. Streiffer, L. Q. Chen, S. W. Kirchoefer, J. Levy, and D. G. Schlom, Nature **430**, 758 (2004).
[3] H. Mizoguchi, H. W. Eng, and P. M. Woodward, Inorg. Chem. **43**, 1667 (2004).
[4] K. Balamurugan, N. Harish Kumar, J. Arout Chelvane, and P. N. Santhosh, J. Alloys Compd. **472**, 9 (2009).
[5] K. Balamurugan, N. Harish Kumar, B. Ramachandran, M.S. Ramachandra Rao, J. Arout Chelvane, and P. N. Santhosh, Solid State Commun. **149**, 884 (2009).
[6] S. J. Pearton, W. H. Heo, M. Ivill, D. P. Norton, and T. Steiner, Semicond. Sci. Technol. **19**, R59 (2004).
[7] JCPDS, PDF file No. 782500.
[8] Y. Wang, Y. L. Cheng, Y. W. Zhang, H. L. W. Chan, and C. L. Choy, Mater. Sci. Eng. B **99**, 79 (2003).
[9] See http://www.cryst.ehu.es for a description of the Bilbao Crystallographic Server.
[10] *The Raman Effect*, edited by R. S. Krishnan and A. Anderson (Marcel Dekker Inc., New York, 1971), Vol. 1.
[11] Y. M. Xiong, T. Chen, G. Y. Wang, X. H. Chen, X. Chen, and C. L. Chen, Phys. Rev. B **70**, 094407 (2004).
[12] Y. L. Cheng, Y. Wang, H. L. W. Chan, and C. L. Choy, Microelectron. Eng. **66**, 872 (2003).
[13] Y. Wang, N. Chong, Y. L. Cheng, H. L. W. Chan, and C. L. Choy, Microelectron. Eng. **66**, 880 (2003).
[14] V. Kapustianyk, Ya Shchur, I. Kityk, V. Rudyk, G. Lach, L. Laskowski, S. Tkaczyk, J. Swiatek, and V. Davydov, J. Phys.: Condens. Matter **20**, 365215 (2008).
[15] J. Hlavay and G. G. Guilbault, Anal. Chem. **49**, 1890 (1977).
[16] S. Tappe, U. Böttger, and R. Waser, Appl. Phys. Lett. **85**, 624 (2004).
[17] B. Tareev, *Physics of Dielectric Materials* (Mir Publishers, Moscow, 1975).
[18] William A. Maryniak, Toshio Uehara, and Maciej A. Noras, Trek Application Note **1005**, 1 (2003).
[19] P. A. Stampe, R. J. Kennedy, Yan Xin, and J. S. Parker, J. Appl. Phys. **92**, 7114 (2002).
[20] J.-Y. Kim, J.-H. Park, B.-G. Park, H.-J. Noh, S.-J. Oh, J. S. Yang, D.-H. Kim, S. D. Bu, T.-W. Noh, H.-J. Lin, H.-H. Hsieh, and C. T. Chen, Phys. Rev. Lett. **90**, 017401 (2003).
[21] D. H. Kim, J. S. Yang, K. W. Lee, S. D. Bu, T. W. Noh, S.-J. Oh, Y.-W. Kim, J.-S. Chung, H. Tanaka, H. Y. Lee, and T. Kawai, Appl. Phys. Lett. **81**, 2421 (2002).
[22] M. Ivill, M. E. Overberg, C. R. Abernathy, D. P. Norton, A. F. Hebard, N. Theodoropoulou, and J. D. Budai, Solid-State Electron. **47**, 2215 (2003).

[This article is copyrighted as indicated in the article. Reuse of AIP content is subject to the terms at: http://scitation.aip.org/termsconditions. Downloaded to] IP: 130.159.70.209 On: Fri, 05 Dec 2014 10:58:16